AD-A272 132

JA 6934

Extracting Target Features from Angle-Angle and Range-Doppler Images

DTIC
ELECTE
NOV 09 1993
A

Su May Hsu

■ For diffuse targets, features such as shape, size, and motion can be determined from a time series of images from either angle-angle passive telescopes or range-Doppler radars. The extracted target features can then be used for automated target recognition and identification.

An algorithm that uses scene-analysis techniques has been developed to perform the feature extraction. The algorithm first processes the images to suppress noise, then applies a two-dimensional slope operation for edge detection to determine the target boundaries. Next, Hough transforms are used on the target edges to detect straight lines and curves, which are subsequently refined with line and curve fits. Groups of the fitted lines are then examined to form cylinders and cones representing typical target components. After these shapes have been identified, the target configuration, size, location, and attitude can be estimated. The target motion can then be inferred from a time series of attitudes that have been extracted from a sequence of images.

FOR A TARGET with rough surfaces, electromagnetic signals are reflected and returned from scatterers that are distributed over the entire target surface. The resulting imagery, whether angle-angle (passive telescopes) or range-Doppler (radar), will show a diffuse object with surface returns that became apparent along the sensor line of sight (LOS). From such images, the target shape, size, and orientation can be determined from pattern recognition and identification techniques. And, with a time sequence of images, the motion of the target can be estimated from its orientation history.

In the feature-extraction algorithm developed at Lincoln Laboratory, the images are first processed to suppress noise and to smooth the image surface. Edge detection is then performed to determine the target boundaries, and the detected edge points are integrated into line segments to form target shapes. Next, target dimensions and orientations are measured from

the line representation of the target, which is assumed to be axisymmetric.

In this article, examples of target feature extraction are demonstrated for both angle-angle and range-Doppler images. For angle-angle images, target orientation is obtained from the projected elliptical shape of circular components and the projected length of a symmetric body axis. For range-Doppler images, target dimensions are first determined from a sequence of range and Doppler extents that have been extracted from the images. The target aspect-angle history can then be derived from that same sequence of range and Doppler extents (as for angle-angle images) by using the estimated target dimensions.

Image Scene Analysis

The goal of target feature extraction is to obtain shape information. From such information, the size, orientation, and position of a target can be estimated.

Image
↓

```
┌─────────────┐
│    Image    │
│  processing │
└─────────────┘
        ↓
┌─────────────┐
│    Edge     │
│  detection  │
└─────────────┘
        ↓
```

Linear Hough transform (classify lines)				Shape projections (classify forms)		
Single lines	Parallel lines	Intersecting lines	→	Cone (half-angle)	Axis of symmetry	
			→	Cylinder (radius)		

```
┌──────────────┐
│  Elliptical  │
│    Hough     │
│  transform   │
│  (determine  │
│ aspect angle)│
└──────────────┘
        ↓
```
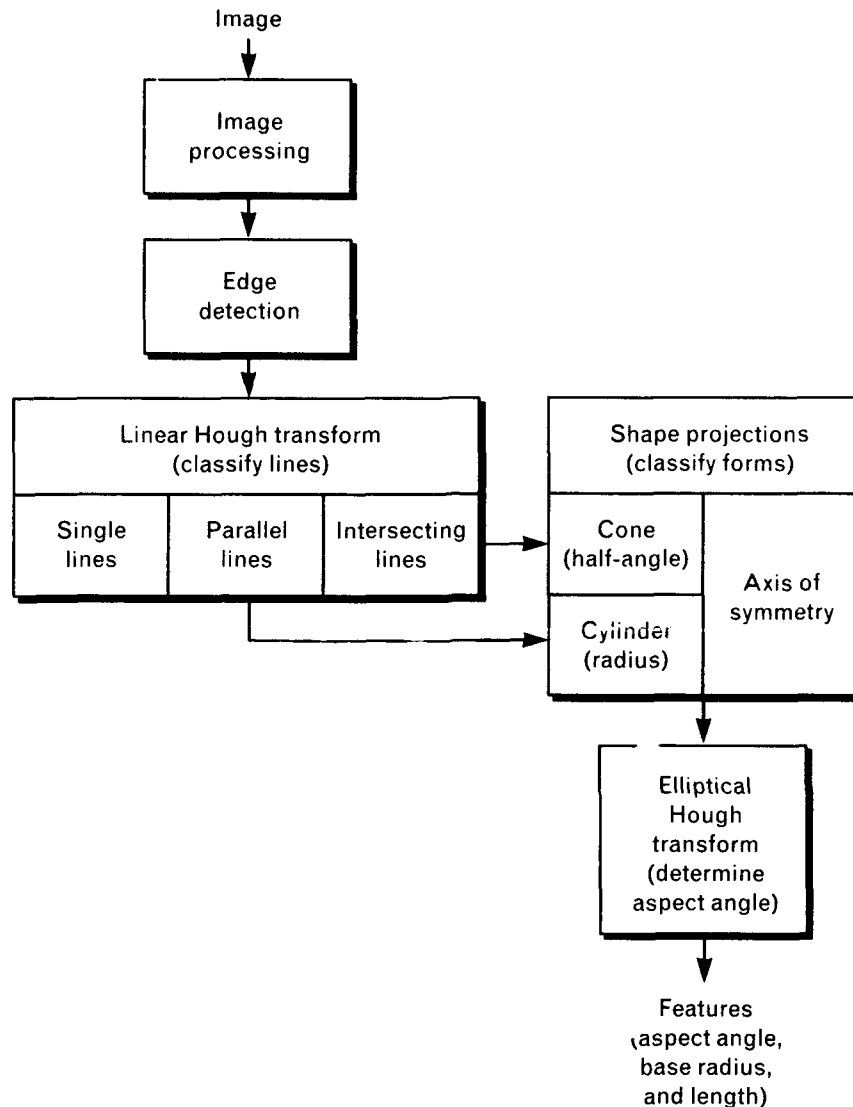
Features
(aspect angle,
base radius,
and length)

FIGURE 1. Feature-extraction process.

Shapes are composed of lines and curves that are collections of boundary edge points. Such edge points can be located with edge-detection techniques. The detected edge points can then be associated with lines and curves by using predetermined fitting constraints. For the current application, cylindrical and conical shapes are considered, and Hough transforms are used to detect the presence of lines and curves [1].

Figure 1 illustrates the feature-extraction process. First, image processing is performed to enhance the edge-detection process. The image processing includes the application of median filters to remove isolated noise, the averaging of multiple image frames to enhance the image signals, and the spatial smoothing of the image surface. Thresholds are then applied to remove the image background. Next, a linear Hough transform is used to detect and collect lines, which are later examined to form the boundaries of cylinders and cones. The position and orientation of the axis of symmetry of each detected shape are then determined. For angle-angle imagery, an elliptical Hough transform is generally used to detect and fit the target-base curve to allow for the subsequent calculation of the target aspect angle. For range-Doppler imagery,

an elliptical Hough transform is used to determine the target dimensions, and, hence, to obtain the target aspect angle.

The three main steps of scene analysis for the extraction of target features are edge detection, line identification, and curve extraction. These three steps are described in the following subsections.

Edge Detection

The boundaries of objects in an image exist at locations where the image values change abruptly. These abrupt changes can be detected by a spatial difference operator [2]. The design of such an operator depends closely on the quality and complexity of the image, and on the desired level of feature extraction. The current application uses spatial gradient operators [3].

The operator center is placed at an image location, and the result of the convolution operation on the image values represents the local gradient at that image location and in the operator's direction. The edge value at the image location $I(x, y)$ can be expressed as

$$G\left[I(x, y)\right] = \sqrt{G_x^2 + G_y^2} ,$$

where G_x and G_y are the image gradients in the horizontal and vertical directions, respectively. The edge is in the gradient direction, which can be obtained as

$$\theta = \tan^{-1} \frac{G_y}{G_x} ,$$

where θ is measured with respect to the x-axis.

Gradient operators of size 5, as shown in Table 1, are used. In general, the operator size should be decreased for coarser image resolutions because, as the resolution becomes coarser, the object boundaries become closer to each other.

The calculated edge values are small for a smooth image surface and large for a discontinuous surface. Thus edge points can be detected by applying a threshold to the edge values. The threshold can be varied, depending on the level of detail desired for edge extraction. The examples presented in this article use a threshold equal to 10% of the dynamic range of the edge values, i.e., $G_{min} + 0.10(G_{max} - G_{min})$. The choice of the threshold, however, can be optimized with respect to the histogram of the edge values. Because of the spatial extent of the operator, the edge values obtained after the application of a threshold generally are thickly populated near or at target discontinuities. Thus a procedure for non-maxima suppression can be applied for the further thinning of these edges [4]. In the procedure, the edge value at a point is set to zero if the value is not the local maximum in the direction perpendicular to the edge direction. Figure 2 shows an example of the detected edge points superimposed over a gray-scaled image. The edge points include the outline of the cones and the silhouette of the cylinder against the background.

Line Identification

After the edge points have been detected, they must be associated with lines and curves. For simple closed contours, the edge points can be chain coded [5], and

Table 1. 5 × 5 Gradient Operators

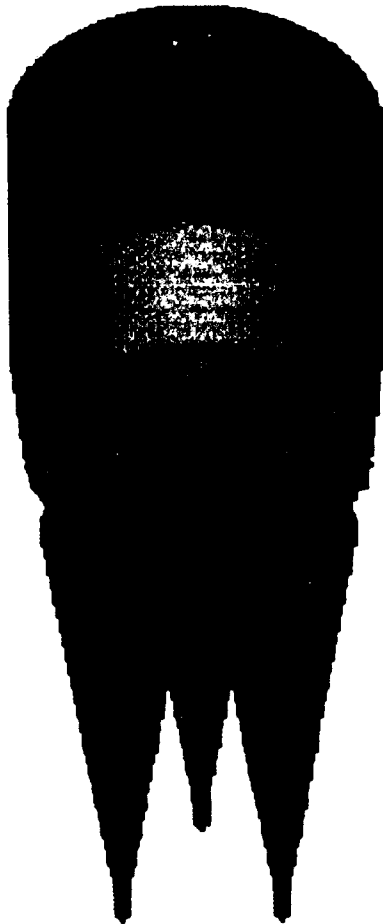| x-Direction					y-Direction				
-2	-2	-2	-2	-2	-2	-1	0	1	2
-1	-1	-1	-1	-1	-2	-1	0	1	2
0	0	0	0	0	-2	-1	0	1	2
1	1	1	1	1	-2	-1	0	1	2
2	2	2	2	2	-2	-1	0	1	2

FIGURE 2. Gray-scaled image with detected edge points.

the shape description can be performed with syntactic pattern grammars [6]. The current application considers images of complex objects comprising a combination of shapes, from which broken edges and edges inside other object boundaries are permitted. Thus a layered approach for shape formation is required.

Hough transforms can be used to detect the lines and curves in an image. In Figure 3(a), a line in two-dimensional (2-D) space is represented by the directed orthogonal distance h to the origin and the angle θ that h forms with the x-axis. Any point (x, y) on the line will satisfy the following equation:

$$h = x \cos \theta + y \sin \theta.$$

The set of lines passing through a given point (x, y) can be plotted in h-θ space. The result will be a sinusoidal curve, as shown in Figure 3(b). Note that

the h curves of two points in x-y space will intersect periodically in h-θ space, and the points of intersection (spaced π radians apart) will correspond to the line defined by the two points in x-y space. Thus, if the h curves of all edge points in an image are plotted in h-θ space, the points at which the h curves intersect will correspond to prominent lines in the image.

In practice, the h-θ space is divided into accumulator cells, and the cell value of a particular cell is increased by 1 each time a curve passes the cell's location. Because the direction of each edge point is known from the edge-detection process (discussed earlier), only the portion of the h curve for angles around that direction needs to be searched. A threshold is chosen at the half-length (in pixels) of the shortest line expected to be extracted from the image. Only those accumulator cells whose cell values are greater than the threshold are selected for further investigation. The selected cells represent a set of lines detected from the image.

For each detected line, a collection of points that lie on the line is gathered from the edge points. To represent the location of a line in the overall image, the mean of the collected points, i.e., the mean (x, y) value, is used. For cases in which several line segments from different image locations happen to be collinear, the line segments will be represented by just single line values of h and θ. In such cases, additional lines—with the same line values h and θ but with different mean (x, y) values—are added to the line set to represent the different line segments. The line set is examined further to eliminate those lines which have mean (x, y) values and h and θ values that are close to other lines. The line set is then used as a set of seeds for growing connected line segments with a relaxation process, as shown in Figure 4.

During each iteration of the relaxation process, each edge point in the image is classified in association with one of the detected lines. The edge point is then added to the point collection of the associated line. When a point is not close enough to any of the lines (the allowable orthogonal distance for point classification should be less than half the distance of the closest distinctive feature lines in the image) or when the edge direction does not agree with the line direction (the allowable angular deviation should be less
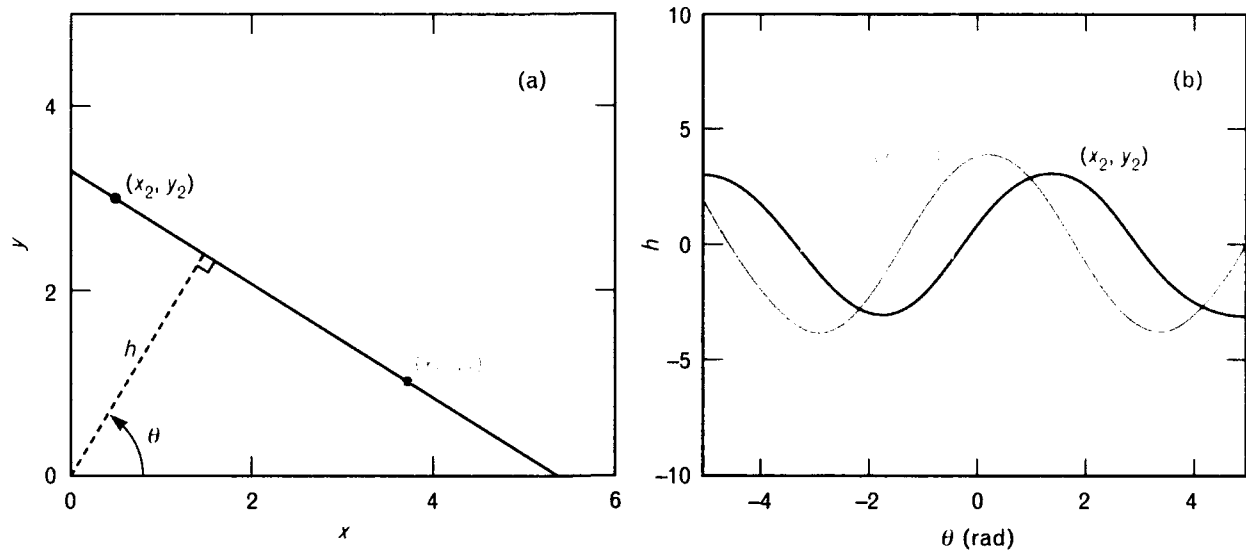
FIGURE 3. Hough transform for straight lines: (a) line defined in x-y coordinates and (b) Hough transform in h-θ space. A line in two-dimensional (2-D) space can be represented by the directed orthogonal distance h to the origin and the angle θ that h forms with the x-axis, as shown in part a. For any given point, the set of lines passing through that point can be plotted in h-θ space. The result will be a sinusoidal curve, as shown in part b. Note that the h curves of two points in x-y space will intersect periodically in h-θ space. The points of intersection (spaced π radians apart) correspond to the line defined by the two points in x-y space.

than half the smallest angle formed by intersecting lines in the image), the point is not classified. At the end of each iteration, the current classification is compared with the results of the previous iteration. If any difference exists, the line set is recalculated from the current point collection and, with the updated line set, the point classification is reiterated. The relaxation process stops when the current classification has not changed from the previous iteration. After the relaxation process ceases, the lines are identified from the edge points, and the position and orientation of each line are calculated from the point collection with a least-squares-error fit. This information is then used for simple shape formation: parallel lines are identified for cylinders, and intersecting lines are chosen for cones. Finally, the axis of symmetry is determined for the position and projected orientation of each chosen shape.

Curve Extraction

The circular base of a cylinder or cone generally appears elliptical in angle-angle imagery because the aspect angle between the object body axis and the

receiver LOS is usually nonzero. From geometry, the ratio of the minor and major axes of the projected ellipse is the cosine of the aspect angle. The aspect angle, together with the projected body-axis orientation, can be used to determine the body attitude with respect to the sensor in 3-D space. In extracting the elliptical base, it is assumed that the straight boundaries have already been identified. Thus the ellipse center will lie on the axis of symmetry of the shape. For cylinders, the major axis of the base ellipse will be half the distance between the two parallel edges that define the shape. For cones, the major axis will be the distance from one conical edge to the ellipse center. Thus the ellipse-extraction scheme first determines the base center along the axis of symmetry of the shape and then fits an elliptical curve at the base region to estimate the minor axis.

Figure 5(a) depicts a cone shape with an elliptical base. The ellipse function with a coordinate rotation β_r is expressed by

$$\frac{(x - x_0)_r^2}{a^2} + \frac{(y - y_0)_r^2}{b^2} = 1 . \tag{1}$$

Line detection from
Hough transformation

↓

Line
calculation/
elimination

↓

Edge-point
classification

↓

Any
changes
from
previous
iteration? — Yes →

↓ No

Group
parallel/
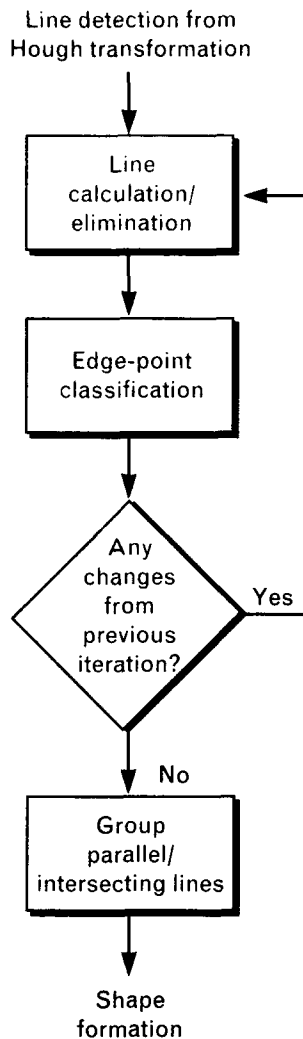intersecting lines

↓

Shape
formation

FIGURE 4. Relaxation process for line identification.

where (x_0, y_0) represents the ellipse center on the axis of symmetry having orientation β_r, and a and b are the minor and major axes of the ellipse, respectively. Equation 1 can be rewritten for the minor axis a:

$$a = \frac{\left|(x - x_0)_r\right|}{\sqrt{1 - \frac{(y - y_0)_r^2}{b^2}}}.$$

The above equation indicates that the minor axis of the ellipse is a function of the location of the ellipse center (x_0, y_0) along the axis of symmetry, as shown in Figure 5(b). Thus the Hough transform space $[a, (x_0, y_0)]$ can be used for ellipse detection in which

values of a are plotted for all edge points in the base region. The maximally accumulated cell in Hough transform space will then determine a and the location of (x_0, y_0).

In addition, the edge detection of a point on the ellipse curve should be consistent with the curve tangent derived by differentiating Equation 1, as follows:

$$\tan \theta = \frac{d(x - x_0)_r}{d(y - y_0)_r} = -\frac{a^2}{b^2} \frac{(y - y_0)_r}{(x - x_0)_r}.$$

Thus each edge point is checked with respect to location and edge orientation before being added to the collection of points for an extracted curve. The minor-axis value is then refined from the best curve fit of the collected points. The results of line and curve identification are shown and discussed in the following section.

Feature Extraction for Angle-Angle Images

For angle-angle imagery, targets are projected from 3-D space to a plane perpendicular to the sensor LOS, as shown in Figure 6. Thus spheres are projected as circles, and the circular bases of cones and cylinders become ellipses. In the images, the physical radii of the circular forms of targets are generally preserved without transformations: the major and minor axes of the elliptical projection are respectively the circular radius itself and the radius with a $\cos\alpha$ factor, α being the aspect angle (i.e., the angle between the target body axis and the sensor LOS). The boundary lines of targets are projected into lines in images, but their dimensions are generally transformed with a factor of $\sin\alpha$. With the use of such projection relationships between target 3-D space and image 2-D space, the size, shape, and orientation of a target can be inferred from its image features.

Two examples of simulated angle-angle images have been analyzed to demonstrate the extraction of target features from such imagery. First, a simulated image of a complex object is used for size and shape estimation. Then a sequence of cone images is employed for motion extraction.

Size and Shape Estimation
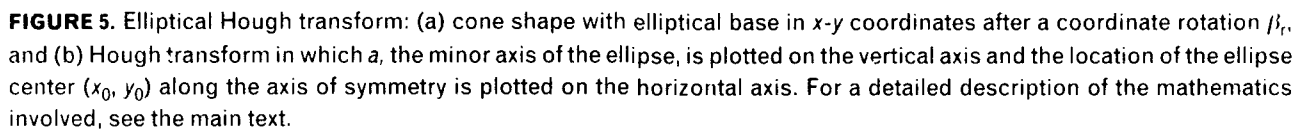
The model used in the example has a cylindrical main

FIGURE 5. Elliptical Hough transform: (a) cone shape with elliptical base in x-y coordinates after a coordinate rotation β_r, and (b) Hough transform in which a, the minor axis of the ellipse, is plotted on the vertical axis and the location of the ellipse center (x_0, y_0) along the axis of symmetry is plotted on the horizontal axis. For a detailed description of the mathematics involved, see the main text.

body with three cones mounted at the forward end. Figure 7(a) shows a simulated angle-angle image of the object at a 50° aspect angle, and Figures 7(b), (c), and (d) show the results of a scene analysis that was performed with pixel sizes of 2, 8, and 20 cm, respectively. For each of the scene-analysis images, the edge points have been detected and lines identified. (Note: The different lines are coded in different colors.) Ideally, two major parallel lines would be selected for the cylindrical body, and three pairs of intersecting lines would be chosen for the cones. Then an elliptical curve could be fitted for the cylindrical base to determine the aspect angle. Because the cylindrical body is large compared to all three of the pixel sizes used, the two parallel lines representing the shape are easily discernible in Figures 7(b), (c), and (d). But the cones, because of their smaller size, appear distorted in the images, particularly in Figure 7(d). Nonetheless, the cones are recognizable at pixel sizes of 2 and 8 cm.

Figure 8 shows the quantitative results. For all pixel sizes, the estimated cylinder radius (Figure 8[a]) agrees well with the model. Estimations for the cone radius (Figure 8[b]) and projected cone angle (Figure 8[c]) are good for pixels smaller than 8 cm, and the aspect

FIGURE 6. Geometry of angle-angle imagery of a cone.
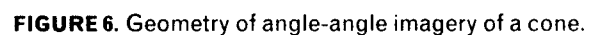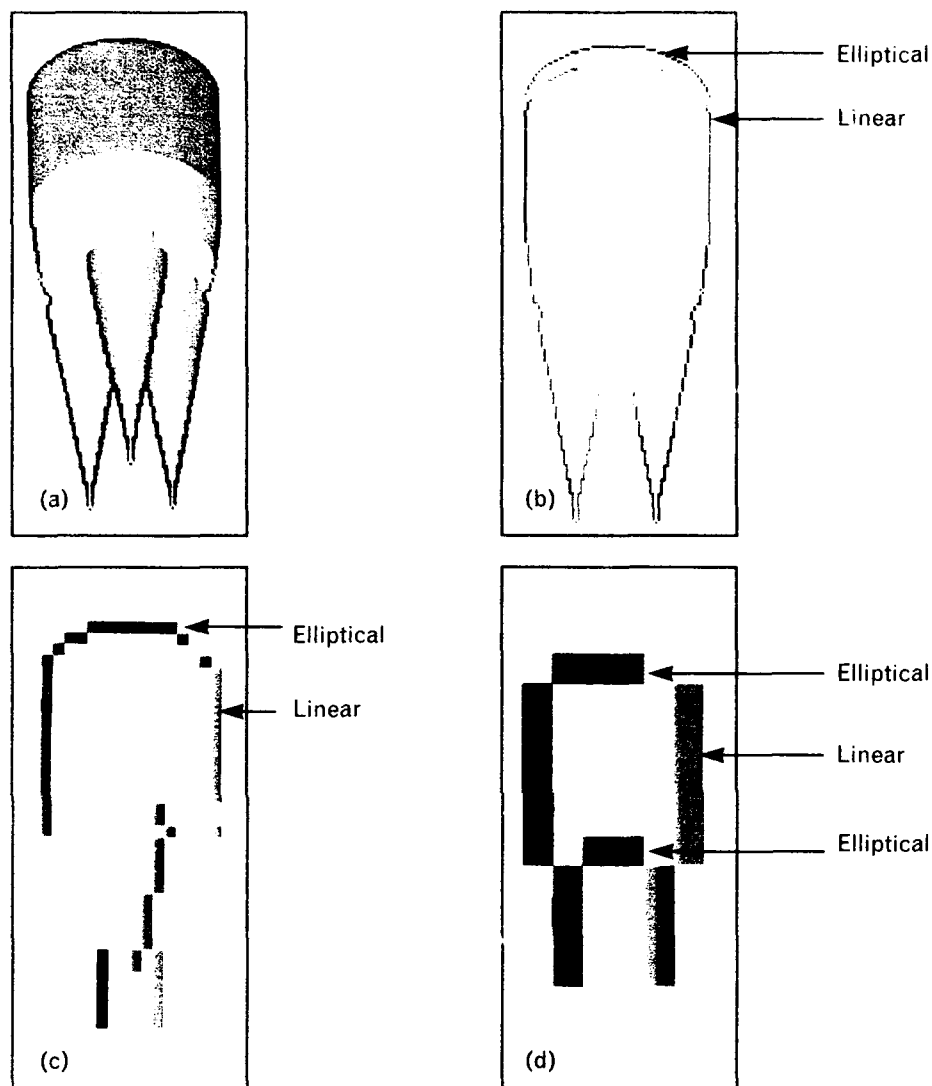
FIGURE 7. Size and shape extraction for a simulated object consisting of a cylindrical main body with three cones mounted at the forward end: (a) angle-angle input image after edge detection, (b) line classification at a pixel size of 2 cm, (c) line classification at a pixel size of 8 cm, and (d) line classification at a pixel size of 20 cm.

angle obtained from the elliptical-curve fit (Figure 8[d]) is also in agreement with the model for pixels smaller than 8 cm.

In general, curve fitting requires finer image quality than line fitting. Lines can usually be detected within one pixel to the true edge. The pixel size, which represents the sampling size at the image focal plane, is determined by the type of focal plane and the angular resolution, the diffraction or resolution limit of the imaging system, and the signal-to-noise

ratio for the target at the receiver.

Motion Extraction

Target motion can be used to aid the target-classification process, as has been demonstrated in range-Doppler imagery from millimeter-wave (MMW) and other microwave radars. With a time series of target attitudes extracted from such imagery, target motion can be inferred. The observation generally is more straightforward in a time series of high-resolution images.
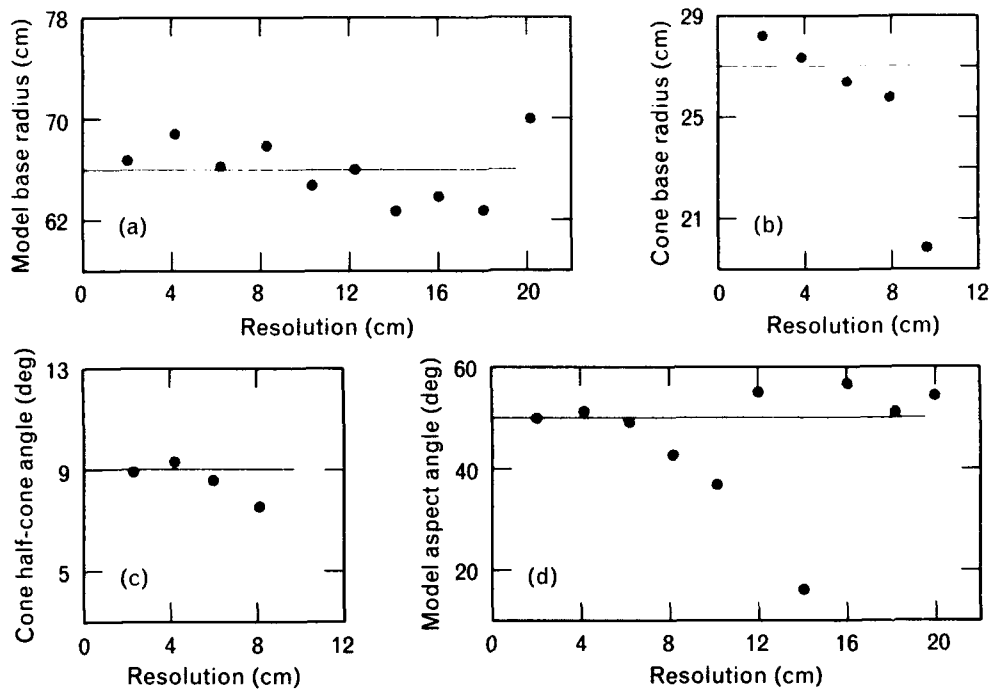
FIGURE 8. Feature-extraction performance at various pixel sizes for the simulated model of Figure 7: (a) calculated base radius of the model, (b) calculated base radius of a cone, (c) calculated half-cone angle of a cone, and (d) calculated aspect angle of the model. (Note: For comparison, the input values used in the simulation are indicated with straight lines.)

For purposes of demonstration, a free-body spin-precession motion is considered. Figure 9 shows a coordinate system with a spinning target and the body axis of the target precessing around the z-axis. The parameters θ_p, ϕ_p, and ρ represent the precession half-cone angle, the precessing azimuthal angle, and the angle between the LOS and the z-axis, respectively. Suppose that ρ and θ_p are constant during an observation. Then the aspect angle α between the body axis and the LOS will be a function of ϕ_p. For ρ in the z-x plane,

$$\cos \alpha = \sin \rho \sin \theta_p \cos \phi_p + \cos \rho \cos \theta_p. \quad (2)$$

If $\cos \alpha$ can be estimated for different values of ϕ_p, then Equation 2 can be used to solve for the coefficients $\sin \rho \sin \theta_p$ and $\cos \rho \cos \theta_p$. The sum and difference of these coefficients are $\cos(\rho - \theta_p)$ and $\cos(\rho + \theta_p)$, respectively, and, from these two quantities, ρ and θ_p can be obtained.

The target projected orientation θ_0 in angle-angle images is also a function of ϕ_p:
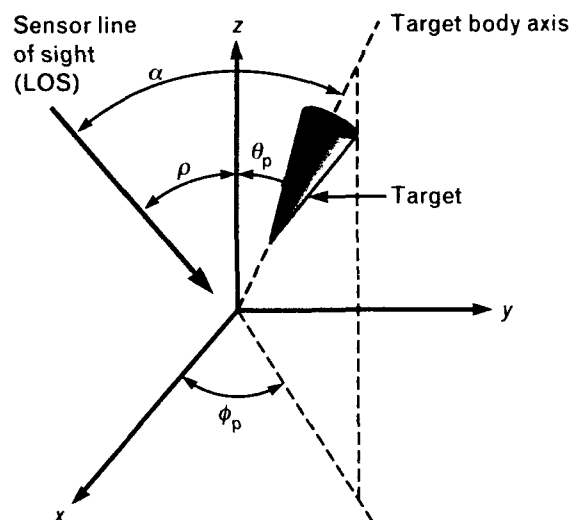
FIGURE 9. Geometry of a target that is spinning (about the target body axis) and precessing (about the z-axis) simultaneously. The parameters θ_p and ϕ_p represent the precession half-cone angle and the precessing azimuthal angle, respectively, and α and ρ represent the aspect angle and mean aspect angle, respectively.

$\varphi_p = 0°$ $\varphi_p = 240°$

(a)   (b)

$\rho = 91.4°$
$\theta_p = 15.4°$
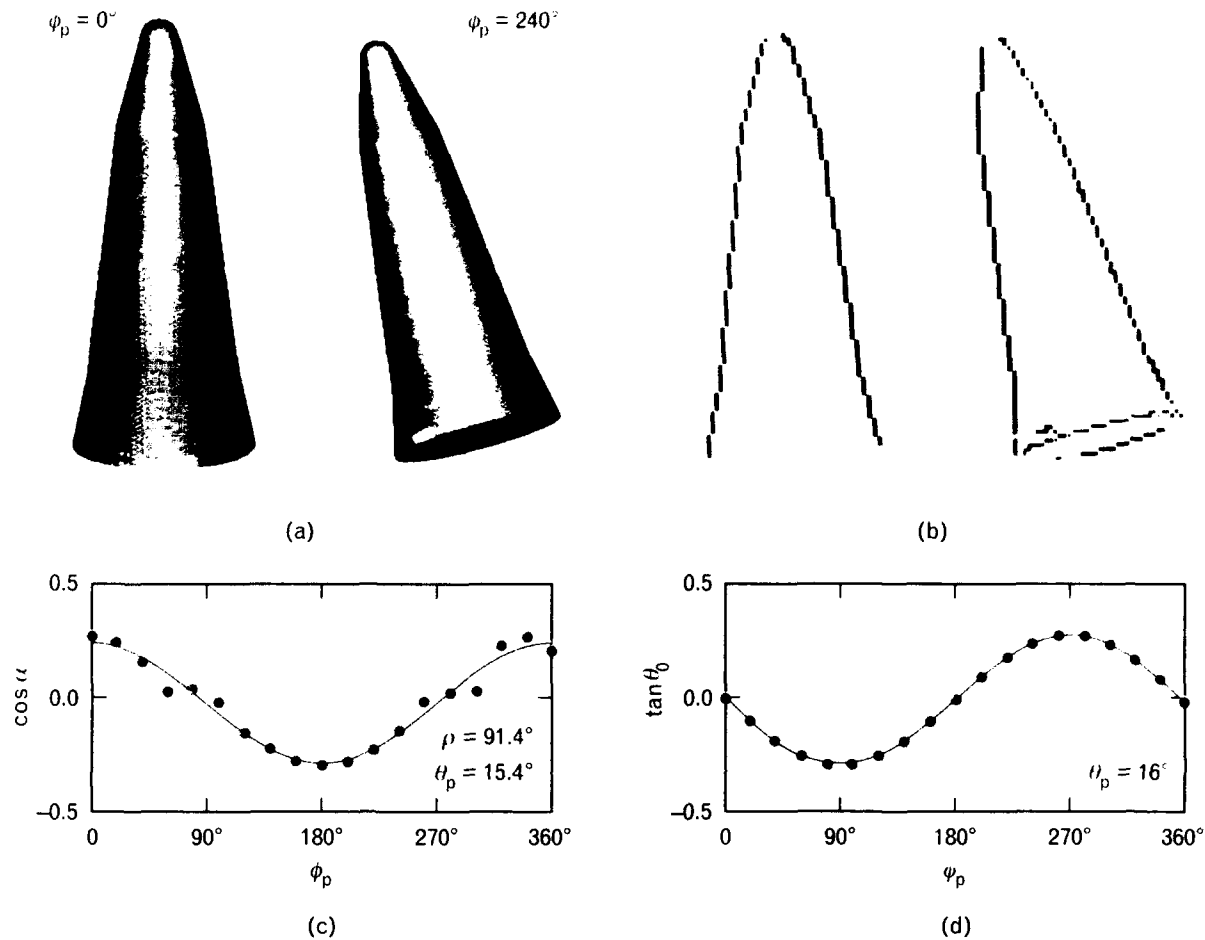
$\theta_p = 16°$

(c)   (d)

FIGURE 10. Feature extraction for angle-angle images of a simulated spinning triconic body undergoing precessional motion: (a) input images, (b) edge extraction, (c) fitted data for $\cos \alpha$, and (d) fitted data for $\tan \theta_0$. The rotation rate chosen was 80°/sec, θ_p was 16°, the precession rate for ϕ_p was 10°/sec, and ρ was 90°. The images were simulated with a 2-cm pixel size and a 2-sec frame time (i.e., a 2-sec interval between frames), with 19 frames generated over a complete precessional cycle.

$4\pi D f_r \sin \alpha$

Invisible (occluded) portion of object

Sensor line of sight (LOS)

Range

Doppler

0

$L \cos \alpha$
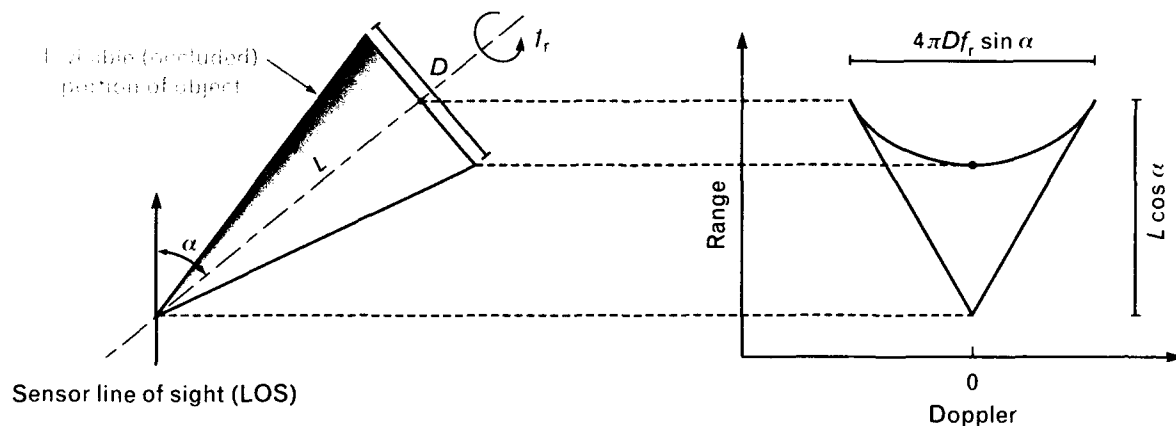
FIGURE 11. Geometry of range-Doppler radar imagery of a spinning cone.

$$\tan \theta_0 = \frac{\sin \theta_p \sin \phi_p}{\cos \rho \sin \theta_p \cos \phi_p - \sin \rho \cos \theta_p}. \qquad (3)$$

At broadside viewing ($\rho = 90°$), Equation 3 reduces to $\tan\theta_0 = -\tan\theta_p \sin\phi_p$. Similar to the case of aspect-angle data, the orientation data can also be fitted with Equation 3 to determine ρ and θ_p.

As an example, a series of simulated angle-angle images has been generated for a spinning triconic body undergoing precessional motion (Figure 10[a]). The rotation rate chosen was 80°/sec, θ_p was 16°, the precession rate for ϕ_p was 10°/sec, and ρ was 90°. (Note: The LOS was assumed to be outside the precession cone.) The images were simulated with a 2-cm pixel size and a 2-sec frame time (i.e., a 2-sec interval between frames), with 19 frames generated over a complete precessional cycle. The triconic boundaries were identified by computer for each image frame (Figure 10[b]) so that the aspect angle α and orientation θ_0 could be determined. Fitting these angles to Equations 2 and 3 then allows ρ and θ_p to be obtained. For the aspect-angle history, Figure 10(c) shows that the best fit occurs for $\rho = 91.4°$ and $\theta_p = 15.4°$. For the image-plane body-axis orientation (given $\rho = 90°$), Figure 10(d) shows that the best fit occurs for $\theta_p = 16°$.

Feature Extraction for Range-Doppler Images

For range-Doppler radars, targets with angular dynamics are imaged along the radar LOS in the two dimensions of range and Doppler. The projection of L, the length of a target measured along its body axis, onto the LOS is $L\cos\alpha$ in the range dimension, with α being the aspect angle, as shown in Figure 11. In the case of a rotating target, the rotational angular velocity V projected onto the LOS is measured in the Doppler dimension as $V\sin\alpha$ [7]. With these relationships, the dimensions of a target can be derived from its image range and Doppler extents.

Application of this technique is demonstrated in this section with an example of simulated range-Doppler images of a diffuse cone. In the example, image processing and scene analysis are applied, as has been demonstrated earlier for angle-angle imagery. A target line model is then used to guide the formation of a target line representation in the imagery. Target di-

mensions and orientations are then determined from the range and Doppler extents of a sequence of the images.

Estimation of Target Dimensions

For the cone-shaped target of Figure 11, the range and Doppler extents are related to the target aspect angle α and the rotation rate f_r by

$$R \cdot dr = L \cos \alpha \qquad (4)$$

and

$$V \cdot dv = 4\pi D f_r \sin \alpha. \qquad (5)$$

where R and V are the range and Doppler extents (number of image pixels), dr and dv are the range and Doppler cell sizes, and L and D are the target physical length and base diameter, respectively. Combining the two equations to eliminate functions of the aspect angle gives the following ellipse equation for a rigid target undergoing steady rotation with constant L, D, and f_r:

$$\left(\frac{d}{L}\right)^2 R^2 + \left(\frac{dv}{4\pi D f_r}\right)^2 V^2 = 1. \qquad (6)$$

The major and minor axes of the above ellipse can be estimated for a dataset of (R, V) pairs by the least-squares-error method. The physical length L and the Doppler velocity can thus be calculated by

$$L = \sqrt{\frac{\overline{R^4 V^4} - \left(\overline{R^2 V^2}\right)^2}{\overline{R^2 V^4} - \overline{V^2} \; \overline{R^2 V^2}}} \; dr$$

and

$$4\pi D f_r = \sqrt{\frac{\overline{R^4 V^4} - \left(\overline{R^2 V^2}\right)^2}{\overline{R^4 V^2} - \overline{R^2} \; \overline{R^2 V^2}}} \; dv.$$

For cases in which the rotation frequency f_r is known, the base diameter D can also be determined from the Doppler velocity. Theoretically, the above derivation can be performed for any dataset with more than two pairs of (R, V) measurements, provided that the data noise or measurement errors are
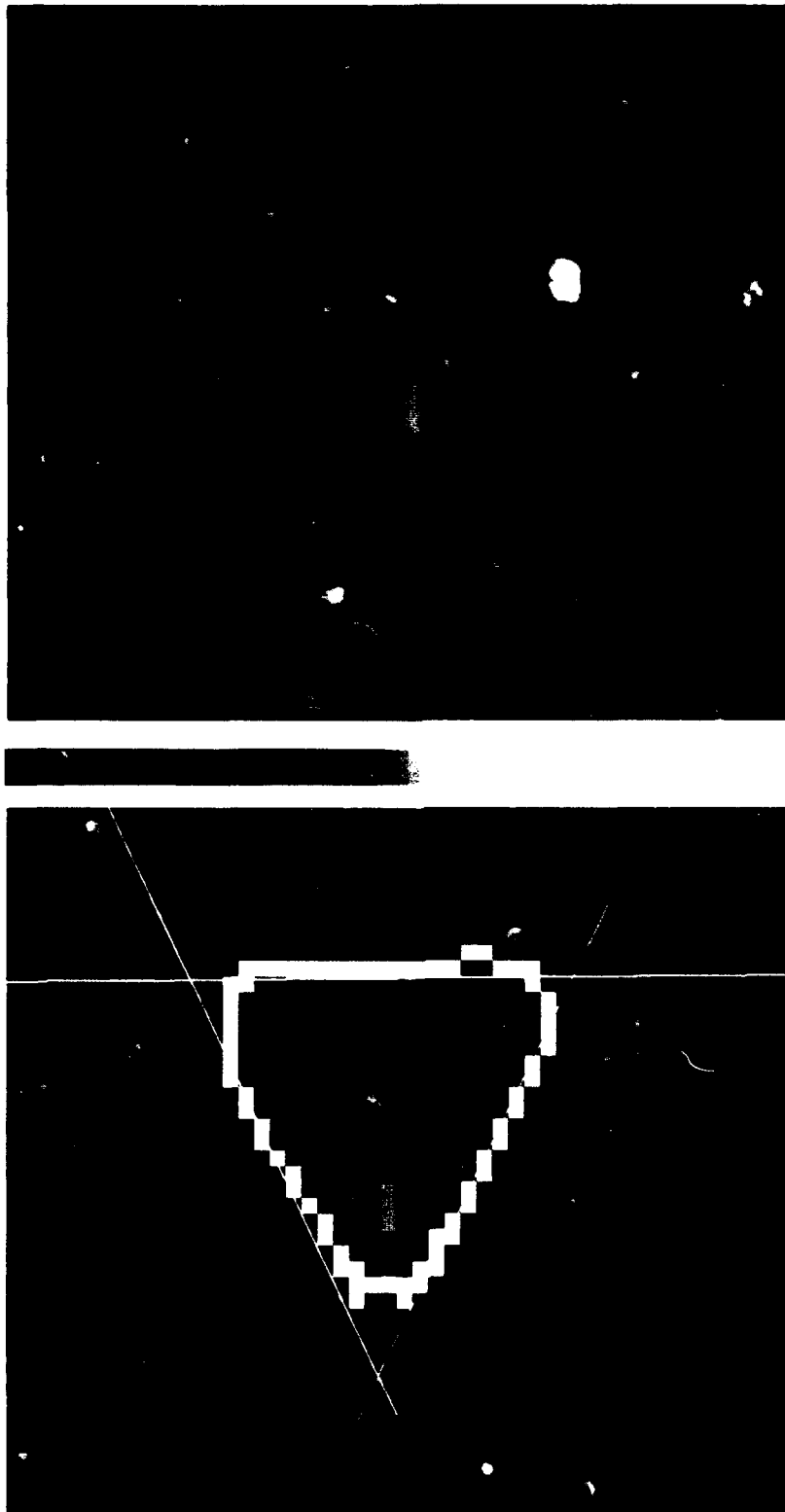
FIGURE 12. Simulated range-Doppler image of a cone: (top) before processing and (bottom) after edge points have been detected and lines fitted. The co'or bar indicates increasing (from black to white) radar cross sectio

much less than the true data difference corresponding to different aspect angles. For a large dataset, the measurements of range and Doppler extents can be median filtered separately to remove noise (while still retaining the temporal trend resulting from changing aspect angles).

With both L and D_f derived from a given dataset, the target aspect-angle history can be obtained from either Equation 4 or 5, or from the ratio of the two equations. It should not matter which equation is used to obtain the aspect angle because both of the equations were used to derive Equation 6, which was used to estimate both L and D_f. More precise results, however, may be obtained by using the equation corresponding to better cell resolution.

Motion Extraction for a Simulated Cone

For purposes of demonstration, range-Doppler images have been simulated for a cone (length of 150 cm and a base radius of 19.7 cm) having a diffuse target surface. A total of 280 images was generated over 28 sec with the cone undergoing spin (spin period of 4.5 sec) and precession [8]. Each image was 53 × 53 pixels, with a range cell representing 5 cm and a Doppler cell representing 2.93 cm/sec. Figure 12 (top) shows one of the range-Doppler image frames.

Image processing, edge detection, and line fitting were then performed on the images. For the simple known target shapes in the current application, the line fitting was simplified with a piecewise linear fitting of the target boundaries: the edges at the base were collected and fitted linearly, and the cone was defined by two lines fitting the cone edges and the base line. Range and Doppler extents of the target could then be estimated from the target line model. Figure 12 (bottom) shows a frame of the image with the edge points detected and the lines fitted. For such figures, the bisection line of the cone is the target-body centerline, the distance from the nose to the base center in range is the target range extent, and the Doppler spread between the intersections of the base line and the cone's left and right sides is the Doppler extent.

Figure 13 contains plots of the extracted range and Doppler extents from the image sequence. Note that, in spite of the considerable amount of local noise
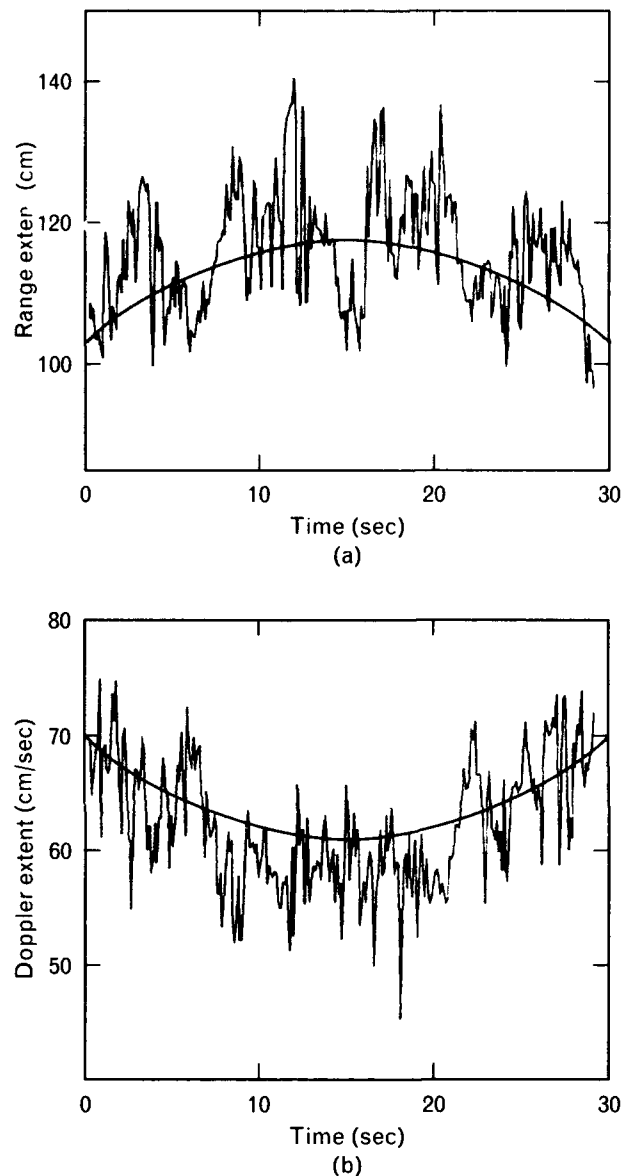

FIGURE 13. The extracted (a) range and (b) Doppler extents from a sequence of simulated images (see Figure 12).

present in the imagery, the range and Doppler histories show functions of $\cos\alpha$ and $\sin\alpha$, respectively, for the aspect angle α, which changes because of the precession of the target. Target dimensions can be obtained by the elliptical fitting of the range and Doppler data, as described earlier in the subsection "Estimation of Target Dimensions." With such techniques, a value of 153.5 cm was calculated for the target length, and 17.3 cm for the base radius. Note that the derived target dimensions agree well with the
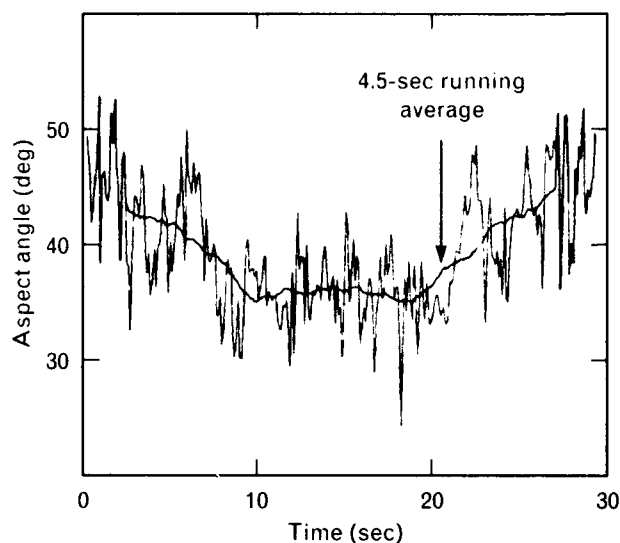
FIGURE 14. Aspect-angle history derived from the Doppler extents (see Figure 13[b]).

For simple known targets, the feature-extraction process can be simplified greatly by obtaining the target image description with a piecewise linear approximation of the target boundaries. For cases in which some size/shape parameters such as cone half-angle, length, and/or base diameter are available, the target size and aspect angle can be estimated from data extracted for each frame of range-Doppler images. Convergence of such estimations over multiple frames of images can then be used to evaluate the algorithm performance and to verify measurements for the known target.

The algorithm is undergoing extensive testing with simulated and field data, and both the precision and efficiency of the algorithm are expected to improve over time. Preparation for real-time implementation of the range-Doppler algorithm is currently in progress.

Acknowledgments

corresponding input model dimensions of 150 cm and 19.7 cm. Both image-resolution-related noise and target-surface-scattering noise could have contributed to the differences in the derived and input target dimensions. The quantitative impacts of such noise are currently under evaluation.

Figure 14 shows the aspect-angle history that was derived from the Doppler extents. A running averaging of 4.5 sec was applied to smooth the aspect-angle curve, which changes from 38° to 47° with a period of about 28 sec. With the assumption that the radar LOS was outside the target precession cone, the target precession half-cone angle can be calculated as 4.5°, which is comparable to the input angle of 5°.

Summary

The extraction of target features—shape, size, orientation, and dynamics—from both angle-angle and range-Doppler images has been demonstrated. The target shape, size and orientation can be determined from single-frame angle-angle images, and the target angular dynamics can be estimated from a time series of such images. For the case of range-Doppler imagery, multiple frames of images are required to obtain multiple measurements of range and Doppler extents to enable the derivation of the target dimensions. A time series of range-Doppler images can also be used to estimate the target angular dynamics.

REFERENCES

1. D.H. Ballard, "Generalizing the Hough Transform to Detect Arbitrary Shapes," *Pattern Recognition* **13**, 111 (1981).
2. R.C. Gonzalez and P. Wintz, "Digital Image Processing," 2nd ed. (Addison-Wesley Publishing Co., Reading, MA, 1987).
3. P.R. Beaudet, "Rotationally Invariant Image Operators," *Proc. Intl. Conf. on Pattern Recognition* (Kyoto, 7–10 Nov. 1978), p. 579.
4. L.S. Davis, "Two-Dimensional Shape Representation," *Handbook of Pattern Recognition and Image Processing*, eds. T.Y. Young and K.S. Fu (Academic Press, Inc., Orlando, FL, 1986).
5. H. Freeman, "On the Encoding of Arbitrary Geometric Configurations," *IEEE Trans. Elec. Computers* **EC-10**, 260 (1961).
6. K.S. Fu, ed., *Syntactic Pattern Recognition, Applications* (Springer-Verlag, Berlin, 1977).
7. A.M. Aull, R.A. Gabel, and T.J. Goblick, "Real-Time Radar Image Understanding: A Machine-Intelligence Approach," *Linc. Lab. J.* **5**, 195 (1992).
8. T.B. Copie, private communication (Oct. 1992).

SU MAY HSU
received the following degrees in electrical engineering: a B.S. from the National Taiwan University and a Ph.D. from Purdue University, where her research focus was in syntactic pattern recognition. She later joined the Corporate Research and Development Center of General Electric Co. in Schenectady, New York, where she became involved in image processing and scene analysis in application to nondestructive part inspection for quality assurance. In 1981 she joined Lincoln Laboratory, where she is currently a staff member in the Signature Studies and Analysis Group, and her focus of research has been in scene analysis and signal processing.

REPORT DOCUMENTATION PAGE

1. AGENCY USE ONLY (Leave blank)	2. REPORT DATE 1993	3. REPORT TYPE AND DATES COVERED JOURNAL ARTICLE

4. TITLE AND SUBTITLE
EXTRACTING TARGET FEATURES FROM ANGLE-ANGLE AND RANGE-DOPPLER IMAGES

6. AUTHOR(S)

SU MAY HSU

5. FUNDING NUMBERS

C — F19628-90-C-0002
PE —

7. PERFORMING ORGANIZATION NAME(S) AND ADDRESS(ES)

Lincoln Laboratory, MIT
P.O. Box 73
Lexington, MA 02173-9108

8. PERFORMING ORGANIZATION REPORT NUMBER

JA-6934

9. SPONSORING/MONITORING AGENCY NAME(S) AND ADDRESS(ES)

US ARMY STRATEGIC DEFENSE COMMAND-HUNTSVILLE
SENSORS DIRECTORATE
P.O. BOX 1500
HUNTSVILLE, AL 35807-3801

10. SPONSORING/MONITORING AGENCY REPORT NUMBER

ESC-TR- 93-297

11. SUPPLEMENTARY NOTES

12a. DISTRIBUTION/AVAILABILITY STATEMENT

Approved for public release; distribution is unlimited.

12b. DISTRIBUTION CODE

13. ABSTRACT

■ For diffuse targets, features such as shape, size, and motion can be determined from a time series of images from either angle-angle passive telescopes or range-Doppler radars. The extracted target features can then be used for automated target recognition and identification.

An algorithm that uses scene-analysis techniques has been developed to perform the feature extraction. The algorithm first processes the images to suppress noise, then applies a two-dimensional slope operation for edge detection to determine the target boundaries. Next, Hough transforms are used on the target edges to detect straight lines and curves, which are subsequently refined with line and curve fits. Groups of the fitted lines are then examined to form cylinders and cones representing typical target components. After these shapes have been identified, the target configuration, size, location, and attitude can be estimated. The target motion can then be inferred from a time series of attitudes that have been extracted from a sequence of images.

14. SUBJECT TERMS
RANGE-DOPPLER IMAGES; ANGLE-ANGLE IMAGES; SCENE ANALYSIS
FEATURE EXTRACTION; HOUGH TRANSFORMATIONS

15. NUMBER OF PAGES
15

16. PRICE CODE

17. SECURITY CLASSIFICATION OF REPORT Unclassified	18. SECURITY CLASSIFICATION OF THIS PAGE Unclassified	19. SECURITY CLASSIFICATION OF ABSTRACT Unclassified	20. LIMITATION OF ABSTRACT